

# Prominent Electron Transport Property Observed for Triply Fused Metalloporphyrin Dimer: Directed Columnar Liquid Crystalline Assembly by Amphiphilic Molecular Design

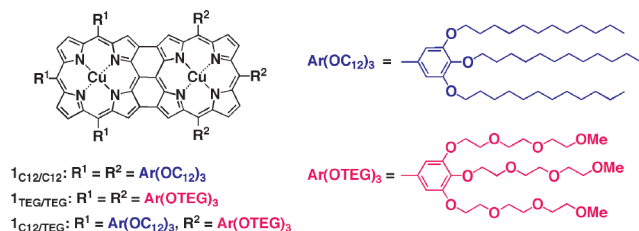
Tsuneaki Sakurai,<sup>†</sup> Keyu Shi,<sup>†</sup> Hiroshi Sato,<sup>†</sup> Kentaro Tashiro,<sup>\*,†</sup> Atsuhiko Osuka,<sup>‡</sup> Akinori Saeki,<sup>§</sup> Shu Seki,<sup>§</sup> Seiichi Tagawa,<sup>§</sup> Sono Sasaki,<sup>⊥</sup> Hiroyasu Masunaga,<sup>⊥</sup> Keiichi Osaka,<sup>⊥</sup> Masaki Takata,<sup>⊥</sup> and Takuzo Aida<sup>\*,†</sup>

School of Engineering and Center for NanoBio Integration, The University of Tokyo, 7-3-1 Hongo, Bunkyo-ku, Tokyo 113-8656, Japan, Graduate School of Science, Kyoto University, Kyoto 606-8502, Japan, Institute of Scientific and Industrial Research, Osaka University, 8-1 Mihogaoka, Ibaraki, Osaka 567-0047, Japan, and Japan Synchrotron Radiation Research Institute/SPRING-8, Sayo-gun, Hyogo 679-5198, Japan

Received May 1, 2008; E-mail: aida@macro.t.u-tokyo.ac.jp; tashiro@macro.t.u-tokyo.ac.jp

Organic semiconductors have attracted increasing attention in view of their potential for low-cost alternatives to amorphous silicon and design flexibility for elaborate electronic devices.<sup>1</sup> In particular, liquid crystalline (LC) semiconductors composed of large  $\pi$ -conjugated molecules are attractive in that their columnar assembly could provide an anisotropic electrical pathway for charge carriers. Moreover, LC materials are solution-processable into large-area thin devices.<sup>2</sup> Representative examples include LC assemblies of large  $\pi$ -conjugated molecules such as triphenylenes,<sup>3b</sup> hexabenzocoronenes,<sup>4</sup> perylene diimides,<sup>5</sup> porphyrins,<sup>3b</sup> and phthalocyanines,<sup>3</sup> where a molecule with a larger  $\pi$ -conjugated core tends to show a higher charge-carrier mobility.<sup>6</sup> Here we report the first LC material of a fused metalloporphyrin dimer (**1**<sub>C12/TEG</sub>; Chart 1) that displays a top-class intrinsic electron transport property among those reported for *n*-type LC semiconductors. Triply fused metalloporphyrin dimers are a new class of extra-large  $\pi$ -conjugated molecules and potentially interesting for organic electronics. However, the reported crystal packing diagrams mostly adopt a T-shaped molecular geometry,<sup>7a</sup> which is unfavorable for electrical conduction. According to a common strategy for liquid crystallization, we initially incorporated paraffinic (C<sub>12</sub>) side chains into the periphery of a triply fused copper porphyrin dimer (**1**<sub>C12/C12</sub>; Chart 1). However, this strategy failed to give any ordered structures. We then prepared compound **1**<sub>TEG/TEG</sub> having hydrophilic triethylene glycol (TEG) chains and, just for curiosity, amphiphilic **1**<sub>C12/TEG</sub>. Quite interestingly, only **1**<sub>C12/TEG</sub> formed a room-temperature columnar liquid crystal.

## Chart 1



Differential scanning calorimetry (DSC) of **1**<sub>C12/TEG</sub> displayed a phase transition behavior, where a LC mesophase, on second heating, appeared at  $-17^\circ\text{C}$  and then disappeared at  $99^\circ\text{C}$  to form

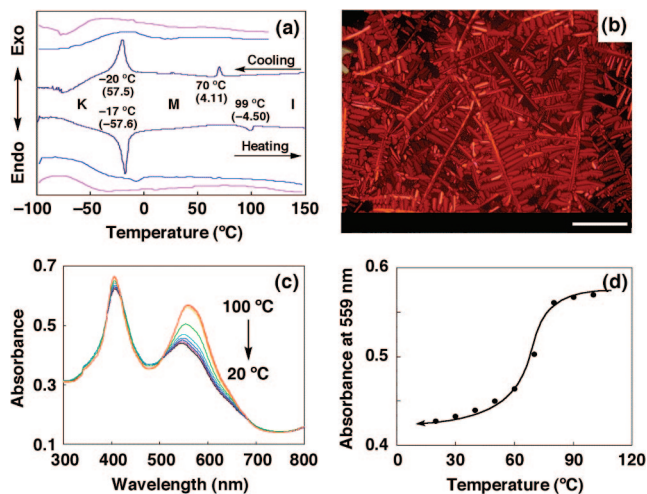


**Figure 1.** (a) DSC traces with phase transition temperatures ( $\Delta H$  values in  $\text{kJ mol}^{-1}$ ) of **1**<sub>C12/TEG</sub> (purple), **1**<sub>C12/C12</sub> (blue), and **1**<sub>TEG/TEG</sub> (pink), on second heating/cooling at  $10^\circ\text{C/min}$ . (b) Polarized optical micrograph of **1**<sub>C12/TEG</sub> at  $50^\circ\text{C}$  (scale bar,  $0.4\text{ mm}$ ). Changes in (c) absorption spectrum and (d) 559-nm absorbance of **1**<sub>C12/TEG</sub> upon cooling from  $100$  to  $20^\circ\text{C}$ .

an isotropic melt (Figure 1a). On cooling from the isotropic melt, the resulting LC mesophase in polarized optical microscopy (POM) showed a clear dendritic texture (Figure 1b)<sup>8</sup> characteristic of columnar LC assemblies. Similar to unassembled **1**<sub>C12/TEG</sub> in  $\text{CHCl}_3$ , the isotropic melt of **1**<sub>C12/TEG</sub> at  $100^\circ\text{C}$  showed two characteristic Soret absorption bands at  $405$  and  $559\text{ nm}$  (Figure 1c).<sup>8</sup> However, when the hot melt was cooled to allow the LC phase transition, the color of the substance changed from dark purple to brown. Accordingly, the longer-wavelength Soret band, on cooling from  $100$  to  $20^\circ\text{C}$ , showed a  $13\text{-nm}$  blue shift (Figure 1c). Furthermore, its absorbance decreased abruptly at the phase transition temperature (Figure 1d). Such a remarkable hypsochromic shift indicates that the columnar mesophase is composed of a  $\pi$ -stacked array of the conjugated core of **1**<sub>C12/TEG</sub>. Meanwhile, a metal-free form of **1**<sub>C12/TEG</sub> displayed a LC mesophase, but the phase transition to an isotropic melt took place at a lower temperature ( $74^\circ\text{C}$ ), suggesting that the high planarity of the copper porphyrin moiety<sup>7a</sup> contributes to the thermal stability of the LC columns of **1**<sub>C12/TEG</sub>. X-ray diffraction (XRD) analysis at  $30^\circ\text{C}$  of the LC assembly of amphiphilic **1**<sub>C12/TEG</sub> showed two distinct diffraction peaks at  $2\theta = 0.79$  and  $1.60^\circ$ , along with minor diffractions in a wider-angle region.<sup>8</sup> Most of these diffractions were successfully indexed to a rectangular columnar lattice with lattice parameters *a* and *b* of  $65.3$

<sup>†</sup> The University of Tokyo.

<sup>‡</sup> Kyoto University.

<sup>§</sup> Osaka University.

<sup>⊥</sup> SPRING-8.

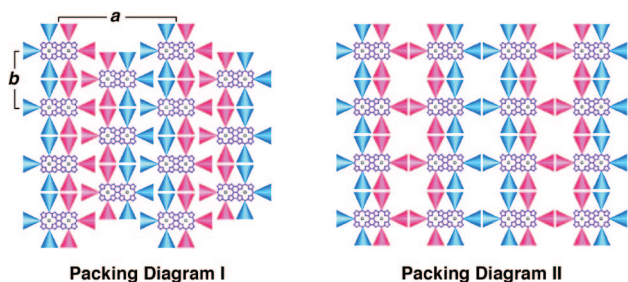


**Figure 2.** Schematic representations of rectangular 2D molecular packing diagrams plausible for liquid crystalline **1**<sub>C12/TEG</sub>.

and 37.2 Å, respectively (Figure 2). In sharp contrast with **1**<sub>C12/TEG</sub>, hydrophobic **1**<sub>C12/C12</sub> and hydrophilic **1**<sub>TEG/TEG</sub> showed neither a phase transition behavior (Figure 1a) nor X-ray diffractions.<sup>8</sup> The absorption spectral patterns of these compounds resembled those in CHCl<sub>3</sub> and remained virtually unchanged over a wide temperature range from 100 to 20 °C.<sup>8</sup>

Why does the amphiphilic molecular design of **1**<sub>C12/TEG</sub> enhance the  $\pi$ -stacking interaction? This is most likely due to a nanoscale phase separation caused by an incompatibility between the hydrophobic and hydrophilic side chains of **1**<sub>C12/TEG</sub>. Figure 2 shows rectangular 2D molecular packing diagrams, which are most plausible in that they involve only a minimum contact between the hydrophobic and hydrophilic nanodomains. Diagram I with a dense molecular packing is considered more likely than diagram II having many vacant sites. In fact, the XRD patterns<sup>8</sup> and lattice parameters, observed for sheared and unsheared samples of liquid crystalline **1**<sub>C12/TEG</sub>, are satisfied only with diagram I. Considering the rectangular lattice geometry, the LC mesophase is most likely formed by piling up this 2D layer on top of each other. When the neighboring 2D layers are disordered along the *a*-axis, the hydrophobic and hydrophilic domains would have to contact one another. Likewise, disordering of the 2D layers along the *b*-axis could destabilize the LC, since unfavorable mixing of the rigid core and flexible side chains would result. Consequently, the  $\pi$ -conjugated core is forced to stack up by this nanoscale phase separation.<sup>8</sup> Again, the amphiphilic molecular design is essential, since mixing of hydrophobic **1**<sub>C12/C12</sub> and hydrophilic **1**<sub>TEG/TEG</sub> resulted in a macroscopic phase separation without any particular structural features.

Square-wave voltammetry of amphiphilic **1**<sub>C12/TEG</sub> in CH<sub>2</sub>Cl<sub>2</sub> showed first oxidation and reduction potentials of 0.25 and −0.90 V vs Fc/Fc<sup>+</sup>, respectively.<sup>8</sup> Similar to reported examples,<sup>7c</sup> the calculated HOMO–LUMO gap of 1.15 V is obviously smaller than those of copper porphyrin monomers (2.2–2.4 V),<sup>7c</sup> and even smaller than those of perylene diimides (1.4–2.2 V)<sup>9</sup> and phthalocyanines (1.4–1.8 V).<sup>10</sup> This feature is quite beneficial for the efficient transport of charge carriers. To evaluate the intrinsic charge-carrier mobility with a minimum grain-boundary effect, we measured the flash-photolysis time-resolved microwave conductivity (FP-TRMC)<sup>11</sup> of the LC state of **1**<sub>C12/TEG</sub>. Upon exposure to a laser pulse of  $\lambda = 355$  nm at 16 °C,<sup>8</sup> the sample showed a prompt rise of a TRMC signal to furnish in 2.6  $\mu$ s a maximum transient conductivity  $\langle \phi \Sigma \mu_{\max} \rangle$  of  $2.4 \times 10^{-4}$  cm<sup>2</sup>/V·s (Figure 3a, red). For the observed TRMC response, the  $\pi$ -stacking of the **1**<sub>C12/TEG</sub> core in the columnar LC assembly is crucial, since an amorphous film of **1**<sub>C12/C12</sub> exhibited  $\langle \phi \Sigma \mu_{\max} \rangle$  of only  $0.3 \times 10^{-4}$  cm<sup>2</sup>/V·s (Figure 3a, blue), which is roughly an order of magnitude smaller than that of liquid crystalline **1**<sub>C12/TEG</sub>. We conducted in situ transient absorption spectroscopy to identify and quantify the charge carrier responsible for the TRMC signal. Upon excitation at 355

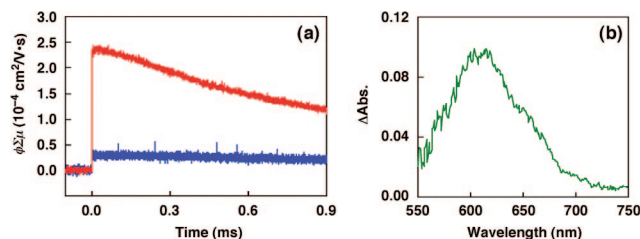


**Figure 3.** (a) FP-TRMC responses of film samples of **1**<sub>C12/TEG</sub> (red) and **1**<sub>C12/C12</sub> (blue), and (b) transient absorption spectrum of a film sample of **1**<sub>C12/TEG</sub> at 16 °C upon photoirradiation at 355 nm.

nm, the LC film of **1**<sub>C12/TEG</sub> showed a transient absorption at 620 nm (Figure 3b), whose rise and decay profiles were nicely correlated with those of the TRMC response.<sup>8</sup> By reference to chemically generated radical anion **1**<sub>C12/TEG</sub><sup>•−</sup> and cation **1**<sub>C12/TEG</sub><sup>•+</sup>,<sup>8</sup> we noticed in the transient absorption spectrum a clear sign of the formation of a radical anion species. Namely, liquid crystalline **1**<sub>C12/TEG</sub> serves as an *n*-type semiconductor. This finding was beyond our expectation, while the first reduction potential (−0.90 V) of **1**<sub>C12/TEG</sub> is close to that of C<sub>60</sub> (−1.06 V),<sup>12</sup> a representative *n*-type semiconductor. From the  $\langle \phi \Sigma \mu \rangle$  value in TRMC along with the quantity of photochemically generated **1**<sub>C12/TEG</sub><sup>•−</sup>, the one-dimensional electron mobility  $\mu_{1D}$  of the LC film was evaluated<sup>8,11</sup> as 0.27 cm<sup>2</sup>/V·s at 16 °C. Noteworthy, this is the largest electron mobility among those reported for room-temperature columnar LC materials, studied by TRMC.<sup>5</sup>

While amphiphilic design has been utilized for obtaining 2D lamellar structures,<sup>13</sup> the present work demonstrated that it is useful for constructing 1D columnar structures. Since high-performance *n*-type organic semiconductors are very rare,<sup>14</sup> the prominent electron transport capability, unveiled for  $\pi$ -stacked **1**<sub>C12/TEG</sub>, is noteworthy. Along with an easy tunability of the redox properties by central metal ions, the new LC semiconductor with a large absorptivity for visible light has the potential for solution-processable photovoltaic materials.

**Supporting Information Available:** Synthesis and analytical data of **1**<sub>C12/TEG</sub>, **1**<sub>C12/C12</sub>, and **1**<sub>TEG/TEG</sub>. This material is available free of charge via the Internet at <http://pubs.acs.org>.

## References

- (1) (a) Forrest, S. R.; Thompson, M. E. *Chem. Rev.* **2007**, *107*, 923. (b) Menard, E.; Meitl, M. A.; Sun, Y.; Park, J.-U.; Shir, D. J.-L.; Nam, Y.-S.; Jeon, S.; Rogers, J. A. *Chem. Rev.* **2007**, *107*, 1117.
- (2) (a) Murphy, A. R.; Fréchet, J. M. J. *Chem. Rev.* **2007**, *107*, 1066. (b) Funahashi, M.; Zhang, F.; Tamaoki, N. *Adv. Mater.* **2007**, *19*, 353.
- (3) (a) van Nostrum, C. F.; Picken, S. J.; Schouten, A.-J.; Nolte, R. J. M. *J. Am. Chem. Soc.* **1995**, *117*, 9957. (b) Warman, J. M.; van de Craats, A. M. *Mol. Cryst. Liq. Cryst.* **2003**, *396*, 41.
- (4) (a) Watson, M. D.; Fechtenkötter, A.; Müllen, K. *Chem. Rev.* **2001**, *101*, 1267. (b) Piris, J.; Debije, M. G.; Watson, M. D.; Müllen, K.; Warman, J. M. *Adv. Funct. Mater.* **2004**, *14*, 1047.
- (5) An, Z.; Yu, J.; Jones, S. C.; Barlow, S.; Yoo, S.; Domercq, B.; Prins, P.; Siebbeles, L. D. A.; Kippelen, B.; Marder, S. R. *Adv. Mater.* **2005**, *17*, 2580.
- (6) van de Craats, A. M.; Warman, J. M. *Adv. Mater.* **2001**, *13*, 130.
- (7) (a) Tsuda, A.; Furuta, H.; Osuka, A. *Angew. Chem., Int. Ed.* **2000**, *39*, 2549. (b) Tsuda, A.; Osuka, A. *Science* **2001**, *293*, 79. (c) Fendt, L.-A.; Fang, H.; Plonska-Brzezinska, M. E.; Zhang, S.; Cheng, F.; Braun, C.; Echegoyen, L.; Diederich, F. *Eur. J. Org. Chem.* **2007**, *28*, 4659.
- (8) See Supporting Information.
- (9) Lee, S. K.; Zu, Y.; Herrmann, A.; Geerts, Y.; Müllen, K.; Bard, A. J. *J. Am. Chem. Soc.* **1999**, *121*, 3513.
- (10) Lever, A. B. P.; Minor, P. C. *Inorg. Chem.* **1981**, *20*, 4015.
- (11) Saeki, A.; Seki, S.; Koizumi, Y.; Sunagawa, T.; Ushida, K.; Tagawa, S. *J. Phys. Chem. B* **2005**, *109*, 10015.
- (12) Xie, Q.; Arias, F.; Echegoyen, L. *J. Am. Chem. Soc.* **1993**, *115*, 9818.
- (13) For review, see: Tschierske, C. *J. Mater. Chem.* **2001**, *11*, 2647.
- (14) Francesco, B.; Farinola, G. M.; Naso, F.; Ragni, R. *Chem. Commun.* **2007**, *10*, 1003.

JA8030714